European Journal of Medicinal Chemistry 112 (2016) 280–288

Contents lists available at ScienceDirect

European Journal of Medicinal Chemistry

journal homepage: http://www.elsevier.com/locate/ejmech

Research paper

Design, synthesis, and structure-activity relationship study of glycyrrhetinic acid derivatives as potent and selective inhibitors against human carboxylesterase 2

Li-Wei Zou [a], Yao-Guang Li [a], Ping Wang [a], Kun Zhou [a, b], Jie Hou [d], Qiang Jin [a], Da-Cheng Hao [c], Guang-Bo Ge [a, *], Ling Yang [a, e, **]

[a] Laboratory of Pharmaceutical Resource Discovery, Dalian Institute of Chemical Physics, Chinese Academy of Sciences, Dalian, 116023, China
[b] College of Pharmacy, Liaoning University of Traditional Chinese Medicine, Dalian, 116600, China
[c] School of Environment and Chemical Engineering, Dalian Jiaotong University, Dalian, 116028, China
[d] Dalian Medical University, Dalian, 116044, China
[e] Jiangxi University of Traditional Chinese Medicine, Nanchang, 330004, China

ARTICLE INFO

Article history:
Received 9 October 2015
Received in revised form
4 February 2016
Accepted 5 February 2016
Available online 9 February 2016

Keywords:
Glycyrrhetinic acid
Structure-activity relationship
Human carboxylesterase 2
Selective inhibitor

ABSTRACT

Human carboxylesterase 2 (hCE2), one of the major carboxylesterases in the human intestine and various tumour tissues, plays important roles in the oral bioavailability and treatment outcomes of ester- or amide-containing drugs or prodrugs, such as anticancer agents CPT-11 (irinotecan) and LY2334737 (gemcitabine). In this study, 18β-glycyrrhetinic acid (GA), the most abundant pentacyclic triterpenoid from natural source, was selected as a reference compound for the development of potent and specific inhibitors against hCE2. Simple semi-synthetic modulation on GA was performed to obtain a series of GA derivatives. Structure-activity relationship analysis brought novel insights into the structure modification of GA. Converting the 11-oxo-12-ene of GA to 12-diene moiety, and C-3 hydroxyl and C-30 carboxyl group to 3-O-β-carboxypropionyl and ethyl ester respectively, led to a significant enhancement of the inhibitory effect on hCE2 and the selectivity over hCE1. These exciting findings inspired us to design and synthesize the more potent compound **15** (IC_{50} 0.02 μM) as a novel and highly selective inhibitor against hCE2, which was 3463-fold more potent than the parent compound GA and demonstrated excellent selectivity (>1000-fold over hCE1). The molecular docking study of compound **15** and the active site of hCE1 and hCE2 demonstrated that the potent and selective inhibition of compound **15** toward hCE2 could partially be attributed to its relatively stronger interactions with hCE2 than with hCE1.

1. Introduction

Carboxylesterases (CEs, E.C.3.1.1.1) are members of the serine hydrolase superfamily that cleaves carboxyesters into the corresponding carboxylic acid and alcohol via a proton transfer hydrolysis mechanism by a catalytic Ser-His-Glu triad. These enzymes are widely distributed in metazoan and especially common in mammalian tissues associated with the metabolism of xenobiotics and endobiotics [1–3]. As an important class of phase I metabolizing enzymes in mammals, CEs efficiently mediate the detoxification of environmental toxins and the metabolism of ester compounds [4–6]. In human, most CEs identified to date belong to two isoforms, human carboxylesterase 1 (hCE1) and human carboxylesterase 2 (hCE2) [7]. hCE1 is expressed in many organs, especially in the liver, but its expression in the gastrointestinal tract is markedly low, whereas hCE2 is the major CEs distributed in intestine but at relatively lower level in liver [8–10]. The selective expression of hCE2 in enterocytes may represent a defensive barrier that esterified xenobiotics need to breech before the organism is exposed following ingestion [11]. Thus, hCE2 is considered to be an important modulator of oral ester-containing drugs and other ester-containing xenobiotics during the first-pass metabolism.

Furthermore, hCE2 is the major CE in many tumour tissues and also plays an important role in the treatment outcomes of ester anticancer agents [9,12]. For example, CPT-11 (irinotecan), a

* Corresponding author.
** Corresponding author. Laboratory of Pharmaceutical Resource Discovery, Dalian Institute of Chemical Physics, Chinese Academy of Sciences, Dalian, 116023, China.
E-mail addresses: geguangbo@dicp.ac.cn (G.-B. Ge), yling@dicp.ac.cn (L. Yang).

http://dx.doi.org/10.1016/j.ejmech.2016.02.020
0223-5234/

carbamate prodrug prescribed for the treatment of colorectal cancer, is hydrolyzed by CEs to yield its active form SN-38 (ethyl-10-hydroxy-camptothecin) [13,14]. However, CPT-11 induced delayed diarrhoea is strongly associated with the activation of the prodrug by hCE2 in the small intestine [13,15]. Therefore, it is hypothesized that the co-administration of the potent and selective hCE2 inhibitor may alleviate CPT-11 associated toxicity. Such a strategy could block the hydrolysis of CPT-11 in the human intestine and thus reduce the exposure of intestinal SN-38, which may alleviate CPT-11 associated diarrhoea [16–18]. Therefore, it is highly desirable to find potent and selective hCE2 inhibitors which may have wide applications in either the alleviation of prodrug associated toxicities or increasing the bioavailability of oral ester-containing drugs that are inactivated by hCE2.

Glycyrrhetinic acid (GA), the major bioactive ingredient of the roots and rhizomes of licorice (*Glycyrrhiza* species), is a famous herbal medicine component in both eastern and western countries [19,20]. Over the past decade, GA has been used as an effective structural template in searching for more potent lead compounds with diverse pharmacological properties, such as anti-inflammation, anti-ulcer, anti-tumor, anti-virus, and anti-hepatotoxic activities [21–26]. Despite these sporadic reports, the potential applications of GA and its derivatives for developing novel pharmacological properties are far from being comprehensively exploited. As a safe natural product, the anti-inflammatory and anti-bacterial activities of GA could reduce CPT-11 associated diarrhoea and improve the life quality of irinotecan prescribed patients [27–30]. In recent years, screening of the specific and potent inhibitors toward hCE2 from medicinal plants and their extracts for translational applications has attracted increasing attentions [31–34]. However, to the best of our knowledge, there is no literature concerning with GA and its derivatives in the aforementioned field. Here, we select GA as the scaffold and focus on its structural modifications by the following strategies: (a) building up a 3-one or ester moiety in ring A of GA; (b) converting the 11-oxo-12-ene of GA in ring C to 12-diene moiety; (c) altering the C-30 carboxyl group to ester, amide, or nitrile functionality. The purpose of this study was to explore the detailed structure-activity relationship (SAR) of a series of GA derivatives as hCE2 inhibitors, which was then used to design more potent and selective hCE2 inhibitors based on GA skeleton.

2. Results and discussion

2.1. Chemistry

GA derivative compounds **2**–**13** were synthesized according to Scheme 1. The GA (**1**) was reduced with zinc in the presence of concentrated hydrochloric acid to afford the 11-deoxo compound **2**. 3-Keto compounds **3** and **4** were obtained with the Jones' reagent in high yield from GA and compound **2** respectively. Reaction of the corresponding haloalkane with GA furnished the target compounds **5**–**7**, in over 80% yields. GA was acetylated in C-3 with acetic anhydride in pyridine to obtain ester **9** with high yield (95%). Compound **12** was synthesized from **7** by the same method as compound **9**, with only 37% yield. Compound **9**, the acetate of GA, was then treated with oxalyl chloride without isolation, and further reacted with concentrated ammonia to afford amide **10** in a yield of 94% over two steps. Compound **10** was hydrolyzed by NaOH to afford compound **8** in 90% yield. The 3β-hydroxy group of **6** was reacted with succinic anhydride in the presence of 4-dimethylaminopyridine (DMAP) to obtain the target product **13** in 75% yield.

2.2. SAR study

GA and its derivatives were evaluated for their inhibitory activities against human CEs (including hCE1 and hCE2). The bioassay results are summarized in Table 1. The parent compound GA (**1**) exhibited poor inhibitory effect on those two hCEs. The 11-ketal moiety of the GA, surprisingly, was found to markedly influence the compound inhibitory effect on hCE2. The compound **2**, 11-deoxo-GA derivative, showed promising inhibitory activity against hCE2 with IC_{50} value to be as low as 6.95 μM and 10-fold more efficient than the parent compound, whereas the inhibitory effect toward hCE1 was only slightly increasing. Compounds **3** and **4** exhibited relatively low inhibitory activities against hCEs as compared with GA and compound **2**, respectively, suggesting that the introduction of carbonyl group at C-3 results in a loss of potency. Further modifications to the 30-position including esters, amides and nitriles are listed in Table 1. Esterified compounds **5** and **6**, with small alkyl groups such as methyl and ethyl, are potent selective inhibitors of hCE2 instead of hCE1. Compound **7** bearing a bulky hydrophilic ester showed enhanced inhibitory effect but poor selectivity toward hCE2, in contrast to compounds **5** and **6**. The amide derivative, compound **8**, displayed moderate inhibitory effect on hCE2, and its inhibition against hCE1 was significantly reduced, compared with ester derivatives **5**–**7**. Compound **11** could inhibit neither hCE1 nor hCE2 (IC_{50} > 100 μM), indicating that the nitrile group introduced in such a position is not beneficial for compound inhibitory property toward hCEs. Replacements of the C-3 hydroxyl group with ethyl ester in compounds **9** and **10** led to an increase of the inhibitory effects on hCE2 and a considerable selectivity toward hCE2 rather than hCE1, as compared with GA and compound **8**. Compound **12** had a similar range of activity as compound **7**, while replacement of the C-3 ethyl ester group with 3-O-β-carboxypropionyl in compound **13** led to a dramatic increase of the inhibitory effect and specificity toward hCE2. Compound **13** exhibited potent inhibitory effect on hCE2 with the relatively low IC_{50} (0.66 μM) and strict selectivity toward hCE2. These results are summarized in Fig. 1 and enable us to better understand the SAR of GA-derived hCE2 inhibitors. The structure modifications of GA, i.e., converting the 11-oxo-12-ene to 12-diene moiety, as well as C-3 hydroxyl and C-30 carboxyl group to 3-O-β-carboxypropionyl and ester respectively, led to a dramatic increase of the inhibitory effect on hCE2 and selectivity over hCE1.

2.3. Design of a novel potent inhibitor

With these SAR results, we next designed and synthesized a novel GA derivative compound **15** that may exhibit more potent and higher selective inhibitory effect on hCE2. The synthetic route is described in Scheme 2. Compound **2** was introduced with ethyl ester in C-30 with ethyl bromide in the presence of potassium carbonate to obtain compound **14**, and its yield was 80%. The 3β-hydroxy group of **14** was reacted with succinic anhydride to harvest the target product **15** in 75% yield. The novel compound **15** showed unusually potent inhibitory activity against hCE2 with much lower IC_{50} value of 0.02 μM and was 3463-fold more potent than the parent compound GA, and it was 1020-fold more selective over hCE1. For comparison, two reported positive inhibitors (BNPP and bavachinin) were tested [34,35]. The result indicated that both compounds showed inferior inhibitory activity and selectivity compared to compound **15**. Furthermore, our results indicated that compound **15** acted as a competitive inhibitor of hCE2 and exhibited a K_i value of 0.042 μM in the human liver microsomes (HLMs) (Supporting Information (SI) Fig. 1). To the best of our knowledge, compound **15** is the most potent hCE2 inhibitor that can work in human tissue preparations. Compound **15** could be

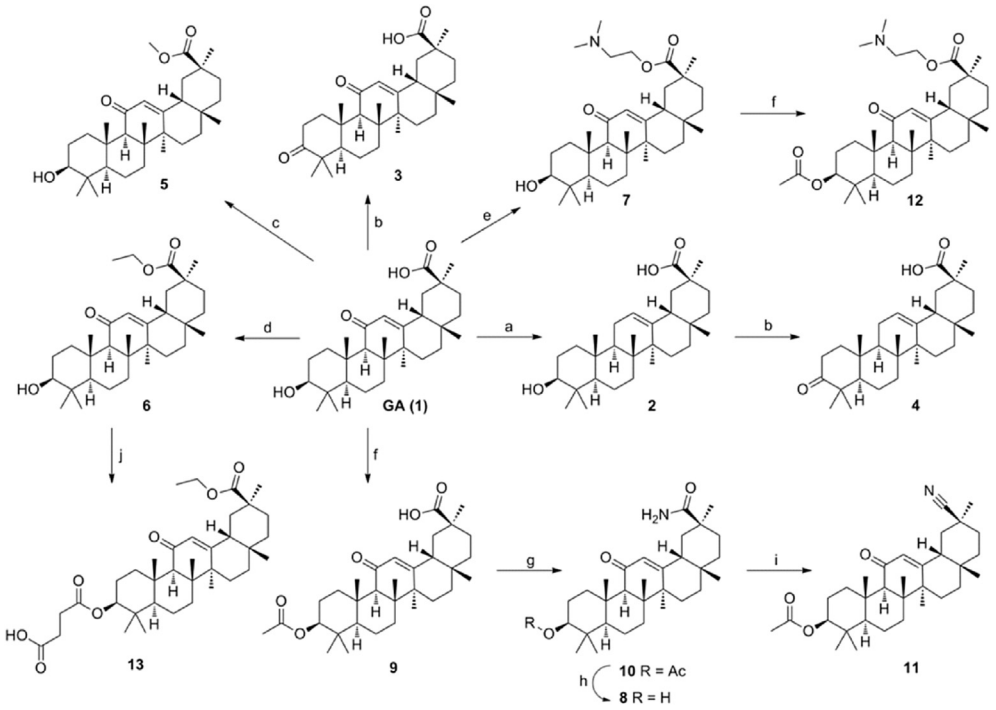

Scheme 1. Synthesis of GA derivatives **2**–**13**, reagents, and conditions: a) Zn, con. HCl aq, dioxane, 10–15 °C, 1 h, 73%; b) Jones reagent, acetone, 0 °C, 1 h, 75–95%; c) CH_3I, K_2CO_3, acetone, rt, 12 h, 81%; d) EtBr, K_2CO_3, acetone, 35 °C, 48 h, 87%; e) 2-Bromo-*N*,*N*-dimethyl ethanaminium bromide, K_2CO_3, acetone, rt, 16 h, 97%; f) acetic anhydride, pyridine, 0 °C, 12 h, 37–95%; g) $(COCl)_2$, CH_2Cl_2, rt, 2 h, then conc. ammonia, toluene, 4–8 °C, 1 h, 94%; h) NaOH, MeOH/THF, 40 °C, 5 h, 90%; i) $SOCl_2$, reflux, 4 h, 72%; j) succinic anhydride, DMAP, CH_2Cl_2, rt, 24 h, 75%.

Table 1
The IC_{50} values of GA and its derivatives toward hCE1 and hCE2.

Compd	IC_{50} (hCE2)[a] μM	IC_{50} (hCE1)[a] μM	IC_{50} (hCE1)/IC_{50} (hCE2)
1	69.26 ± 8.92	20.97 ± 5.70	0.3
2	6.95 ± 0.69	10.53 ± 2.07	1.5
3	>100	>100	–
4	20.75 ± 2.52	23.61 ± 7.71	1.1
5	5.61 ± 2.71	22.36 ± 4.08	4.0
6	5.70 ± 2.44	26.26 ± 7.5	4.6
7	3.95 ± 0.39	9.13 ± 1.58	2.3
8	14.21 ± 1.63	6.99 ± 1.35	0.5
9	40.51 ± 6.86	49.86 ± 16.63	1.2
10	7.36 ± 1.32	10.97 ± 2.77	1.5
11	>100	>100	–
12	3.42 ± 1.16	12.31 ± 3.79	3.6
13	0.66 ± 0.16	>100	>151.5
14	3.99 ± 1.35	25.09 ± 12.32	6.3
15	0.02 ± 0.005	20.41 ± 6.39	1020.5
16[b]	6.11 ± 0.79	0.14 ± 0.02	0.02
17[c]	4.31 ± 0.31	3.47 ± 0.57	0.8

[a] All data presented are averages of at least three separate experiments.
[b] Bis-*p*-nitrophenyl phosphate.
[c] Bavachinin.

applied to selectively modulate the function of hCE2 in complex biological samples.

2.4. Molecular docking

In order to gain a deeper understanding of the selective inhibitory effect of compound **15** on hCE2, molecular docking studies were performed by Surflex-Dock calculations with a crystal structure of hCE1 and an established hCE2 homology model (SI Fig. 2) as the macromolecular models. As shown in Fig. 2, compound **15** can be well docked into the hydrophobic catalytic cavity of both hCE1 and hCE2, and the strong hydrophobic interactions between compound **15** and the key residues of hCE1 and hCE2 could be observed (SI Fig. 2). Compound **15** could interact with two residues in hCE1, i.e., Leu-255 and Thr-252 (Fig. 2), but it was far from the catalytic amino acid Ser-221 (>5 Å). In sharp contrast, more hydrogen bonds could be formed between compound **15** and hCE2 (Gly-149, Lys-308, and Met-354), and the side chain of compound **15** (in C-3 position) could tightly bind with Ser-228 (2.71 Å) via H-bonding. As a result, the bioactive pose of compound **15** in hCE2 got a higher Surflex-Dock score (4.13) than that in hCE1 (−3.60). The strong H-bonding interaction between compound **15** and the catalytic residue of hCE2 (Ser-228) implied that hCE2-mediated hydrolysis might be totally blocked by this compound, and the reason may be that Ser-228 is an essential residue participating in recognition and catalysis of hCE2 substrates. These findings agreed well with the experimental data where compound **15** exhibited much more potent inhibitory effect on hCE2 but a relatively weaker one on hCE1.

3. Conclusions

In summary, we have evaluated the inhibitory effects of a series of glycyrrhetinic acid derivatives against two major human carboxylesterases. The inhibitory activities of synthesized compounds toward hCE2 were in the range of 0.02 μM to more than 100 μM, while their selectivity for hCE2 over hCE1 were in the range of 0.3–1020 folds, spanning nearly four orders of magnitude. Our results demonstrated that the structural modifications of GA, i.e., converting the 11-oxo-12-ene to 12-diene moiety, and C-3 hydroxyl and C-30 carboxyl group to 3-O-β-carboxypropionyl and ethyl ester respectively, could enhance the inhibitory activities against hCE2. On the basis of structure-inhibitory activity relationship, we designed and synthesized a more potent compound **15**

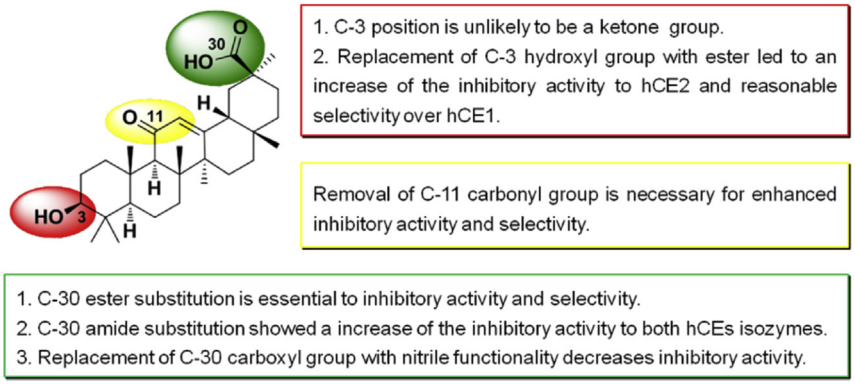

Fig. 1. SAR summary of GA analogues.

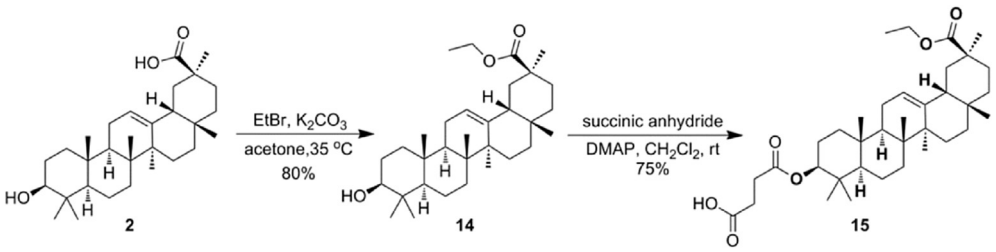

Scheme 2. Synthesis of compound **15**.

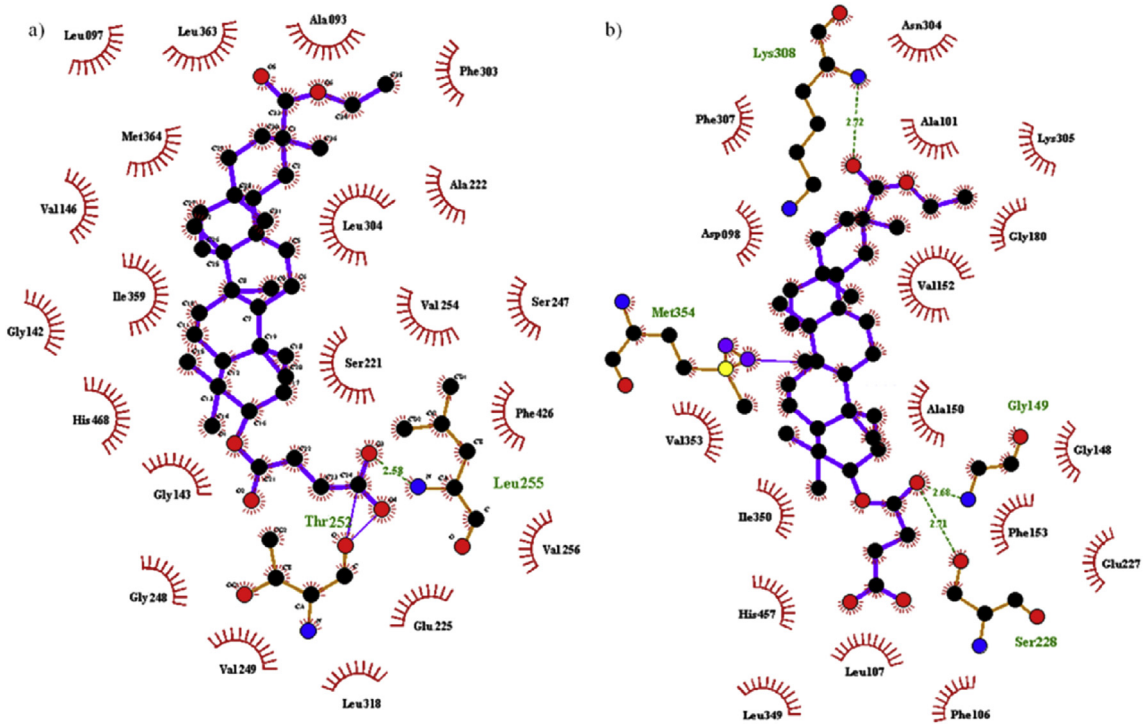

Fig. 2. Schematic drawing of interactions between compound **15** and the active site of hCE1/hCE2. (a) Detailed binding sites of compound **15** in the active site of hCE1; (b) Detailed binding sites of compound **15** in the active cavity of hCE2. The ligand bonds and external bonds are depicted as purple lines. The hydrogen bonds are shown as green dashed lines with indicated bond length, and the residues involved in hydrophobic interactions are shown as red arcs. (For interpretation of the references to colour in this figure legend, the reader is referred to the web version of this article.)

($IC_{50} = 0.02$ μM, $K_i = 0.042$ μM) as a novel and selective inhibitor of hCE2, which was about 3463-fold more potent than the parent compound GA and demonstrated greater than 1020-fold selectivity over hCE1. Additionally, molecular docking revealed the essential structural and chemical features of this GA derivative as a potent hCE2 inhibitor. All these findings will be implicated for the design

and further optimization of potent and highly selective hCE2 inhibitors, which could serve as a promising tool for exploring the biological functions of hCE2 in various biological systems, as well as a promising drug candidate for clinical applications in selectively modulating hCE2-associated toxicities.

4. Experimental

4.1. Chemicals and reagents

Fluorescein Diacetate (FD), Fluorescein and Bis-*p*-nitrophenyl phosphate (BNPP) were purchased from TCI (Tokyo, Japan). 2-(2-Benzoyl-3-methoxyphenyl) benzothiazole (BMBT) was synthesized from 2-(2-hydroxyl-3-methoxyphenyl) benzothiazole (HMBT) as previously reported [36], and its structure was confirmed by ^{1}H NMR, ^{13}C NMR and high resolution mass spectrometry (MS). The purity of FD and BMBT was greater than 98%. Stock solutions of FD (1 mM) and BMBT (1 mM) were prepared in DMSO and stored at −20 °C till use. 18β-Glycyrrhetinic acid was purchased from Chengdu Pufei De Biotech Co., Ltd. (Chengdu, Sichuan, China). The purity of the standard compound was determined by HPLC-UV, which was greater than 98%. The phosphate buffer (pH 7.4) was prepared in Millipore water and stored at 4 °C till use. Millipore water (Millipore, Bedford, USA), HPLC grade acetonitrile, methanol, and formic acid (Tedia company, USA) were employed throughout the study. The pooled HLMs from 50 donors were obtained from Celsis, Inc. (USA) and stored at −80 °C till use. All ^{1}H NMR (400 MHz) and ^{13}C NMR (101 MHz) were recorded on a VARIAN INOVA-400 spectrometer with chemical shifts reported as ppm (in CDCl3, TMS as the internal standard). High resolution MS data were obtained with the LTQ Orbitrap mass spectrometer (Orbitrap Elite).

4.2. Enzyme inhibition assays

The inhibitory effects toward hCEs were investigated with BMBT and FD as the specific probe substrates for hCE1 and hCE2, respectively [36]. In brief, a typical incubation mixture with a total volume of 0.2 mL contained HLMs (2 μg/mL), 0.1 M potassium phosphate (pH 7.4), and GA or its derivatives (100 μM, 10 μM or 1 μM). After 10 min pre-incubation at 37 °C, BMBT (10 μM, final concentration) or FD (15 μM, final concentration) was added to initiate the reaction, with the final concentration of ethanol or DMSO at 1% (v/v, without loss of the catalytic activity). In this study, HLM was employed as the enzyme source, as it is easily available and contains the same level of hCE2 as human intestine microsomes (HIMs) [37,38]. The inhibitory tendency and potency of two esterase inhibitors toward hCE2 in HLM and HIM are similar with FD as the probe substrate [39]. The incubation mixture was incubated at 37 °C for 30 min, then the ice-cold acetonitrile (equal volume of incubation mixture, 0.2 mL) was added to terminate the reaction. The mixtures were centrifuged at 20,000 × g for 10 min. The aliquots of supernatant were retrieved for further LC-UV analysis. The column temperature was kept at 40 °C. Acetonitrile (A) and water with 0.2% formic acid (B) were applied as the mobile phase at a flow rate of 0.4 mL/min, with a gradient: 0–9.0 min, 90% B–5% B; 9.0–12.0 min, 5% B; 12.0–15.0 min, balance to 90% B. BMBT and its hydrolytic metabolite were detected at 300 nm under UV analysis. The negative control incubations (ethanol or DMSO only) and positive control (with a potent CE inhibitor BNPP) were carried out under the same conditions [39]. The residual activities of hCE1 were calculated with the following formula: the residual activity (%) = the peak area of HMBT in the presence of inhibitor/the peak area of HMBT in the negative control × 100%. The residual activities of hCE2 were calculated with the following formula: the residual activity (%) = the florescence intensity in the presence of inhibitor/the florescence intensity in the negative control × 100%. All assays were conducted in triplicate, and the data were shown as mean ± SD.

4.3. Inhibition kinetic analysis

The inhibition behaviors of GA and its derivatives on hCE1 and hCE2 were characterized according to the literature [34]. The concentration of the inhibitor applied when the target enzyme retains half of its catalytic activity (IC_{50}) was determined by various inhibitor concentrations under the incubation conditions described above. Inhibition constant values were determined by varied concentrations of FD in the presence or absence of each inhibitor. To determine the inhibition kinetic types (competitive inhibition, noncompetitive inhibition, or uncompetitive type) of analyzed compounds, multiple concentrations of FD and varied concentrations of inhibitor were utilized to determine the corresponding reaction rates. Dixon plot and Lineweaver-Burk plots were used to fit the data [40]. The inhibition kinetic type was evaluated through determining the intersection point in the Dixon and Lineweaver-Burk plots. The second plot based on the slopes from Lineweaver-Burk plot vs. inhibitor concentrations was utilized to calculate each inhibition constant (K_i) value.

4.4. Statistical analysis

All values obtained from experiments were expressed as mean ± SD. The IC_{50} values were evaluated by nonlinear regression in GraphPad Prism 6.0 software (GraphPad Software, Inc., La Jolla, CA, USA).

4.5. 3D structures of hCE1 and hCE2

The structure of hCE1 was obtained from Protein Data Bank (http://www.rcsb.org/pdb), and the PDB code was 1MX5. The comprehensive crystal structure of hCE2 has not been resolved to date, thus we carried out homology modelling of hCE2 to obtain its three-dimensional structure. The amino acid sequence of hCE2 was retrieved from the Swiss-Prot database (entry code O00748). A three-dimensional structure modelling was carried out in Swiss-Model Automatic Modelling Mode (http://swissmodel.expasy.org/) with the resolved structure of hCE1 set as the template ((PDB ID: 1MX5, resolution 2.0 A°, identity hCE1 vs. hCE2 = 49.71%). Root mean square deviations (RMSD) of the fitted 3-D structures were calculated by PyMol 1.4 package (www.pymol.org). We employed the Protein Structure and Model Assessment Tools available at SWISS-MODEL Workspace (http://swissmodel.expasy.org) to assess the quality of the 3-D models.

4.6. Molecular docking

The Tripos force field was employed to minimize the molecular energy and search for the most stable conformation by the Powell conjugate gradient algorithm with a convergence criterion of 0.001 kcal/mol. The energy gradient limit was set at 0.05 kcal/mol*Å. The partial charges of each compound were calculated by Gasteiger-Huckel method, which were done by SYBYL-X program (Tripos Inc.). Docking of ligands into the catalytic domain of the enzyme model was carried out in Surflex-Dock (within Sybyl-X1.2, Tripos International). The protomol was generated via the automated method, with a threshold of 0.50 and a bloat value of 2, when all other parameters were set to their default values. The Total-Score function was employed to rank the docked compound poses, the top 20 ranked poses for each compound were examined

visually. PyMOL was applied to generate and analyze the illustration of the whole protein-ligand complex [41]. The Surflex-Dock scores are expressed in−log (K_d) units. For the polar and hydrophobic interactions between the protein and the ligand compound **15** or GA, illustrations were generated and the analyses were performed by Ligplot program [42,43].

4.7. General procedures for the synthesis of GA derivatives **2**–**15**

4.7.1. 18β-11-Deoxo-olean-12-en-30-oic acid (**2**)

Zn (536.5 mg, 8.1 mmol, 16.2 equiv) was added to a solution of dioxane (9 mL) and GA **1** (235.3 mg, 0.5 mmol, 1.0 equiv). The mixture was cooled to 10–15 °C and concentrated HCl solution (1.45 mL) was added over a period of 30 min. The reaction was stirred for further 30 min. Progress of the reaction was monitored by TLC. After completion of the reaction, the dioxane was distilled off. The resulting mixture was diluted with water and extracted with dichloromethane (30 mL × 2). The combined organic layers were washed with water (10 mL) and brine (10 mL), and dried over sodium sulfate. After evaporation of the solvent, the crude residue was purified by column chromatography on silica gel (petroleum ether: ethyl acetate = 5: 1) to yield the compound **2** (167.3 mg, 73%) as a white solid. ^{1}H NMR (400 MHz, $CDCl_3$) δ 5.30 (s, 1H), 3.23 (dd, J = 11.2, 4.8 Hz, 1H), 2.02–1.74 (m, 8H), 1.71–1.59 (m, 6H), 1.56–1.48 (m, 2H), 1.46–1.30 (m, 6H), 1.20 (s, 3H), 1.14 (s, 3H), 1.00 (s, 3H), 0.97 (s, 3H), 0.94 (s, 3H), 0.90–0.87 (m, 2H), 0.81 (s, 3H), 0.79 (s, 3H), 0.76–0.73 (m, 1H). ^{13}C NMR (101 MHz) δ 181.2, 144.2, 122.8, 79.1, 55.2, 48.1, 47.7, 44.0, 42.7, 41.5, 39.8, 38.8, 38.6, 38.3, 37.0, 32.7, 32.0, 31.2, 28.7, 28.2, 28.1, 27.2, 27.0, 26.2, 26.0, 23.5, 18.4, 16.8, 15.6, 15.5. HRMS (ESI) Calcd. for $C_{30}H_{47}O_3^-$ ([M − H]$^-$) 455.3576, Found 455.3532.

4.7.2. 18β-3, 11-Dioxo-olean-12-en-30-oic acid (**3**)

Jones reagent (prepared from 107.9 mg of CrO3) was added to a solution of GA **1** (470.1 mg, 1 mmol, 1.0 equiv) in acetone (10 mL) at 0 °C over a period of 30 min till the brown color persisted. The resulting solution was stirred for further 30 min. Progress of the reaction was monitored by TLC. After completion of the reaction, isopropanol (0.5 mL) was added. After evaporation of the solvent, the crude residue was diluted with dichloromethane (100 mL). The organic layer was washed with water (25 mL × 2) and brine (25 mL), and dried over sodium sulfate. The solvent was concentrated under vacuum and the residual solid was recrystallized from methanol/dichloromethane to give the ketone **3** (443.3 mg, 95%) as a white solid. ^{1}H NMR (400 MHz, $CDCl_3$) δ 5.75 (s, 1H), 3.49 (s, 1H), 3.06–2.88 (m, 1H), 2.73–2.56 (m, 1H), 2.45 (s, 1H), 2.42–2.30 (m, 1H), 2.22 (d, J = 10.3 Hz, 1H), 2.10–1.98 (m, 2H), 1.97–1.80 (m, 2H), 1.73–1.43 (m, 8H), 1.38 (s, 3H), 1.36–1.32 (m, 2H), 1.28 (s, 3H), 1.23 (s, 3H), 1.18 (s, 3H), 1.11 (s, 3H), 1.07 (s, 3H), 1.05–0.97 (m, 1H), 0.86 (s, 3H). ^{13}C NMR (101 MHz, CDCl3) δ 217.3, 199.7, 181.7, 169.9, 128.4, 61.1, 55.5, 48.3, 47.8, 45.3, 43.8, 43.3, 40.9, 39.7, 37.7, 36.7, 34.2, 32.1, 31.9, 30.9, 28.6, 28.4, 26.6, 26.4, 23.4, 21.4, 18.8, 18.5, 15.6. HRMS (ESI) Calcd. for $C_{30}H_{45}O_4^+$ ([M+H]$^+$) 469.3312, Found 469.3317.

4.7.3. 18β-3-Oxo-11-deoxo-olean-12-en-30-oicacid (**4**)

The preparation was performed as described above for compound **3**, and the synthesis was initiated from compound **2** (50.0 mg, 0.11 mmol) to produce the ketone **4** (34.2 mg, 75%) as a white solid. ^{1}H NMR (400 MHz, $CDCl_3$) δ 11.02 (brs, 1H), 5.32 (s, 1H), 2.60–2.52 (m, 1H), 2.41–2.34 (m, 1H), 2.05–1.75 (m, 8H), 1.71–1.60 (m, 2H), 168–1.49 (m, 3H), 1.47–1.25 (m, 7H), 1.21 (s, 3H), 1.15 (s, 3H), 1.10 (s, 3H), 1.08 (s, 3H), 1.06 (s, 3H), 1.02 (s, 3H), 0.92–0.86 (m, 1H), 0.83 (s, 3H). ^{13}C NMR (101 MHz, CDCl3) δ 217.8, 182.7, 144.3, 122.6, 55.4, 48.1, 47.5, 46.9, 44.1, 42.6, 41.7, 39.8, 39.3, 38.3, 36.7, 34.2, 32.2, 32.0, 31.1, 28.7, 28.2, 26.9, 26.5, 26.1, 25.9, 23.6, 21.5, 19.6, 16.7, 15.2. HRMS (ESI) Calcd. for $C_{30}H_{47}O_3^+$ ([M+H]$^+$) 455.3478, Found 455.3451.

4.7.4. 18β-11-Oxo-olean-12-en-30-oicacidmethyl ester (**5**)

Anhydrous K_2CO_3 (69.1 mg, 0.5 mmol, 1.0 equiv) and CH_3I (46.7 μL, 0.75 mmol, 1.5 equiv) were added to a stirred solution of GA **1** (235.3 mg, 0.5 mmol, 1.0 equiv) in acetone (10 mL) at room temperature (rt). The resulting solution was stirred for 12 h. Progress of the reaction was monitored by TLC. After completion of the reaction, the acetone was distilled off. The resulting mixture was diluted with water (15 mL) and extracted with dichloromethane (30 mL × 2). The combined organic layers were washed with brine (10 mL) and dried over sodium sulfate. After evaporation of the solvent, the crude residue was purified by column chromatography on silica gel (petroleum ether: ethyl acetate = 3: 1) to obtain the compound **5** (195.1 mg, 81%) as a white solid. ^{1}H NMR (400 MHz, $CDCl_3$) δ 5.66 (s, 1H), 3.69 (s, 3H), 3.23 (dd, J = 10.5, 5.5 Hz, 1H), 2.80 (dt, J = 13.4, 3.5 Hz, 1H), 2.34 (s, 1H), 2.10 (d, J = 3.2 Hz, 1H), 2.05–1.96 (m, 2H), 1.94–1.89 (m, 1H), 1.88–1.77 (m, 1H), 1.73–1.55 (m, 7H), 1.50–1.39 (m, 3H), 1.37 (s, 3H), 1.32–1.20 (m, 5H), 1.15 (s, 3H), 1.14 (s, 3H), 1.13 (s, 3H), 1.01 (s, 3H), 0.99–0.91 (m, 1H), 0.81 (s, 6H), 0.74–0.67 (m, 1H). ^{13}C NMR (101 MHz, CDCl3) δ 200.2, 176.9, 169.2, 128.6, 78.8, 61.8, 55.0, 51.8, 48.4, 45.4, 44.1, 43.2, 41.1, 39.1, 37.8, 37.1, 32.8, 31.8, 31.2, 28.5, 28.3, 28.1, 27.3, 26.5, 26.4, 23.4, 18.7, 17.5, 16.4, 15.6. HRMS (ESI) Calcd. for $C_{31}H_{49}O_4^+$ ([M+H]$^+$) 485.3625, Found 485.3624.

4.7.5. 18β-11-Oxo-olean-12-en-30-oic acidethyl ester (**6**)

Anhydrous K_2CO_3 (69.1 mg, 0.5 mmol, 1.0 equiv) and EtBr (55.9 μL, 0.75 mmol, 1.5 equiv) were added to a stirred solution of GA **1** (235.3 mg, 0.5 mmol, 1.0 equiv) in acetone (10 mL) at rt. The resulting solution was stirred at 35 °C for 48 h. Progress of the reaction was monitored by TLC. After completion of the reaction, the acetone was distilled off. The resulting mixture was diluted with water (15 mL) and extracted with dichloromethane (30 mL × 2). The combined organic layers were washed with brine (10 mL) and dried over sodium sulfate. After evaporation of the solvent, the crude residue was purified by column chromatography on silica gel (petroleum ether: ethyl acetate = 3: 1) to give the compound **6** (217.4 mg, 87%) as a white solid. ^{1}H NMR (400 MHz, $CDCl_3$) δ 5.65 (s, 1H), 4.31–3.96 (m, 2H), 3.23 (dd, J = 10.5, 5.6 Hz, 1H), 2.79 (d, J = 13.4 Hz, 1H), 2.34 (s, 1H), 2.20–1.75 (m, 6H), 1.74–1.52 (m, 6H), 1.50–1.40 (m, 2H), 1.37 (s, 3H), 1.34–1.22 (m, 6H), 1.14 (s, 6H), 1.13 (s, 3H), 1.01 (s, 3H), 0.88–0.83 (m, 1H), 0.82 (s, 6H), 0.74–0.70 (m, 1H). ^{13}C NMR (101 MHz, CDCl3) δ 200.2, 176.4, 169.3, 128.5, 78.8, 61.8, 60.3, 55.0, 48.4, 45.4, 43.8, 43.2, 41.1, 39.1, 37.7, 37.1, 32.8, 31.8, 31.1, 28.6, 28.3, 28.1, 27.3, 26.5, 26.4, 23.4, 18.7, 17.5, 16.4, 15.6, 14.3. HRMS (ESI) Calcd. for $C_{32}H_{51}O_4^+$ ([M+H]$^+$) 499.3781, Found 499.3778.

4.7.6. 18β-11-Oxo-olean-12-en-30-oic acid- (2′-dimethylamino) ethyl ester (**7**)

Anhydrous K_2CO_3 (66.3 mg, 0.48 mmol, 1.2 equiv) and 2-bromo-*N*,*N*-dimethyl ethanaminium bromide (111.8 mg, 0.48 mmol, 1.2 equiv) were added to a stirred solution of GA **1** (188.3 mg, 0.4 mmol, 1.0 equiv) in acetone (10 mL) at rt. The resulting solution was stirred at 35 °C for 6 h. Progress of the reaction was monitored by TLC. After completion of the reaction, the acetone was distilled off. The resulting mixture was diluted with water (15 mL) and extracted with dichloromethane (25 mL × 2). The combined organic layers were washed with brine (10 mL) and dried over sodium sulfate. After evaporation of the solvent, the crude residue was crystallized from dichloromethane, ethyl acetate and methyl *tert*-butyl ether to acquire the compound **7** (210.5 mg, 97%) as a white solid. ^{1}H NMR (400 MHz, $CDCl_3$) δ 5.67 (s, 1H), 4.33 (dt, J = 11.7, 5.8 Hz, 1H), 4.21 (dt, J = 11.7, 5.7 Hz, 1H), 3.23 (dd, J = 10.7, 5.6 Hz, 1H), 2.79 (dd,

J = 10.1, 3.4 Hz, 1H), 2.72 (d, J = 5.1 Hz, 2H), 2.40 (s, 6H), 2.34 (s, 1H), 2.15 (dd, J = 13.4, 3.3 Hz, 1H), 2.09–1.96 (m, 2H), 1.96–1.76 (m, 2H), 1.68–1.59 (m, 5H), 1.51–1.39 (m, 3H), 1.37 (s, 3H), 1.36–1.20 (m, 3H), 1.16 (s, 3H), 1.14 (s, 3H), 1.13 (s, 3H), 1.01 (s, 4H), 0.99–0.85 (m, 2H), 0.82 (d, J = 13.6 Hz, 6H), 0.72–0.69 (m, 1H). ^{13}C NMR (101 MHz, $CDCl_3$) δ 200.3, 176.2, 169.3, 128.6, 78.7, 61.8, 61.5, 57.5, 54.9, 48.2, 45.4, 45.4, 43.99, 43.2, 41.1, 39.1, 37.7, 37.1, 32.8, 31.8, 31.1, 28.5, 28.3, 28.1, 27.3, 26.5, 26.4, 23.4, 18.7, 17.5, 16.4, 15.6. HRMS (ESI) Calcd. for $C_{34}H_{56}NO_4^+$ ([M+H]$^+$) 582.4209, Found 542.4183.

4.7.7. 18β-3-O-Acetyl-11-oxo-olean-12-en-30-oic acid(**9**)

Acetic anhydride (5.0 mL) was added dropwise to a stirred solution of GA **1** (500 mg, 1.06 mmol) in pyridine (7.5 mL) at 0 °C. The resulting solution was stirred at rt for 24 h and then poured into ice water (75 mL), resulting in the compound **9** (519 mg, 95%) as the white solid precipitate. ^{1}H NMR (400 MHz, $CDCl_3$) δ 5.71 (s, 1H), 4.52 (dd, J = 11.5, 4.6 Hz, 1H), 2.80 (d, J = 13.5 Hz, 1H), 2.37 (s, 1H), 2.28–2.10 (m, 2H), 2.06 (s, 3H), 2.04–1.78 (m, 4H), 1.77–1.56 (m, 5H), 1.55–1.38 (m, 5H), 1.37 (s, 3H), 1.23 (s, 3H), 1.17 (s, 3H), 1.13 (s, 3H), 1.10–0.93 (m, 3H), 0.88 (s, 6H), 0.84 (s, 3H). ^{13}C NMR (101 MHz, CDCl3) δ 200.3, 181.8, 171.1, 169.5, 128.4, 80.7, 61.7, 55.0, 48.2, 45.5, 43.8, 43.2, 40.9, 38.8, 38.1, 37.7, 37.0, 32.7, 31.9, 30.9, 28.5, 28.5, 28.1, 26.5, 26.4, 23.6, 23.3, 21.3, 18.7, 17.4, 16.7, 16.4. HRMS (ESI) Calcd. for $C_{32}H_{49}O_5$ ([M+H]$^+$) 513.3575, Found 513.3584.

4.7.8. 18β-3-O-Acetyl-11-oxo-olean-12-en-30-amide (**10**)

Oxalyl-chloride (200 μL, 11.65 mmol) was added dropwise to a solution of compound **9** (200 mg, 0.39 mmol) in dichloromethane (16 mL) at rt. After stirring at rt for 2 h, the solvent was removed under reduced pressure and the residue was dissolved in toluene (10 mL). Then a concentrated ammonia (5 mL) was added at 4–8 °C and the mixture was stirred for further 1 h. The mixture was extracted with dichloromethane (25 mL × 2). The combined organic layers were washed with water (10 mL) and brine (10 mL), and dried over sodium sulfate. After evaporation of the solvent, the crude residue was purified by column chromatography on silica gel (petroleum ether: ethyl acetate = 3: 1) to produce the compound **10** (176 mg, 94%) as a white solid. ^{1}H NMR (400 MHz, $CDCl_3$) δ 5.68 (s, 1H), 5.61 (brs, 1H), 5.35 (brs, 1H), 4.52 (dd, J = 11.6, 4.8 Hz, 1H), 2.80 (dt, J = 13.6, 3.4 Hz, 1H), 2.36 (s, 1H), 2.27–2.16 (m, 1H), 2.12–1.98 (m, 4H), 1.96–1.79 (m, 2H), 1.77–1.57 (m, 6H), 1.54–1.40 (m, 4H), 1.37 (s, 3H), 1.34–1.21 (m, 2H), 1.18 (s, 3H), 1.16 (s, 3H), 1.13 (s, 3H), 1.10–0.92 (m, 3H), 0.92–0.84 (m, 6H), 0.83 (s, 3H). ^{13}C NMR (101 MHz, CDCl3) δ 200.0, 178.5, 171.0, 169.2, 128.5, 80.6, 61.8, 55.0, 48.1, 45.4, 43.7, 43.2, 42.0, 38.8, 38.0, 37.4, 367.0, 32.7, 31.9, 31.5, 29.5, 28.5, 28.0, 26.5, 26.4, 23.6, 23.3, 21.3, 18.7, 17.4, 16.7, 16.4. HRMS (ESI) Calcd. for $C_{32}H_{50}NO_4$([M+H]$^+$) 512.3734, Found 512.3775.

4.7.9. 18β-11-Oxo-olean-12-en-30-amide (**8**)

1 M NaOH aq. (180 μL, 0.18 mmol, 1.5 equiv) was added dropwise to a solution of compound **10** (60.0 mg, 0.12 mmol, 1.0 equiv) in methanol (2 mL) and tetrahydrofuran (1 mL) at rt. The resulting solution was stirred at 40 °C for 5 h. Progress of the reaction was monitored by TLC. After completion of the reaction, the solvent was removed under reduced pressure. The resulting mixture was diluted with water (15 mL) and extracted with dichloromethane (30 mL × 2). The combined organic layers were washed with brine (10 mL) and dried over sodium sulfate. After evaporation of the solvent, the crude residue was purified by column chromatography on silica gel (dichloromethane: methanol = 20: 1) to give the compound **8** (50.8 mg, 90%) as a white solid. ^{1}H NMR (400 MHz, HDMSO) δ 7.13 (brs, 1H), 6.77 (brs, 1H), 5.76 (s, 1H), 5.47 (s, 1H), 4.31 (d, J = 5.2 Hz, 1H), 3.09–2.90 (m, 1H), 2.65–2.53 (m, 1H), 2.31 (s, 1H), 2.10–2.02 (m, 2H), 1.92–1.81 (m, 1H), 1.78–1.47 (m, 6H), 1.45–1.36 (m, 2H), 1.34 (s, 3H), 1.30–1.08 (m, 4H), 1.03 (s, 9H), 0.97–0.93 (m, 2H), 0.91 (s, 3H), 0.74 (s, 3H), 0.69 (s, 3H)· ^{13}C NMR (101 MHz, DMSO) δ 199.6, 178.0, 170.2, 127.9, 77.1, 61.62, 54.6, 48.2, 45.3, 43.4, 43.3, 41.3, 39.2, 39.0, 37.8, 37.1, 32.6, 31.9, 29.1, 28.9, 28.6, 27.4, 26.5, 26.4, 23.5, 18.8, 17.6, 16.6, 16.5. HRMS (ESI) Calcd. for $C_{30}H_{48}NO_3$ ([M+H]$^+$) 470.3629, Found 470.3631.

4.7.10. 18β-3-O-Acetyl-11-oxo-olean-12-en-30-nitrile(**11**)

Compound **10** (100 mg, 0.19 mmol) was dissolved in thionyl chloride (3 mL) and the solution was heated under reflux for 4 h. After the solvent was removed under reduced pressure, the crude residue was purified by column chromatography on silica gel (petroleum ether: ethyl acetate = 6: 1) to give the compound **11** (69 mg, 72%) as a white solid. ^{1}H NMR (400 MHz, $CDCl_3$) δ 5.70 (s, 1H), 4.52 (dd, J = 11.6, 3.6 Hz, 1H), 2.79 (d, J = 13.6 Hz, 1H), 2.43–2.28 (m, 2H), 2.06 (m, 3H), 2.03–1.83 (m, 1H), 1.84–1.54 (m, 8H), 1.51–1.40 (m, 4H), 1.37 (s, 3H), 1.33 (s, 3H), 1.26–1.21 (m, 2H), 1.16 (s, 3H), 1.15 (s, 3H), 1.08.101 (m, 3H), 0.93 (s, 3H), 0.88 (s, 6H). ^{13}C NMR (101 MHz, CDCl3) δ 199.6, 171.0, 167.1, 129.1, 123.4, 80.6, 61.8, 55.0, 48.2, 45.3, 43.2, 42.3, 38.8, 38.1, 37.3, 37.0, 35.2, 32.7, 32.6, 32.0, 28.1, 28.1, 27.3, 26.3, 26.3, 23.6, 23.3, 21.3, 18.7, 17.4, 16.7, 16.4. HRMS (ESI) Calcd. for $C_{32}H_{48}NO_3$ ([M+H]$^+$) 494.3629, Found 494.3634.

4.7.11. 18β-3-O-Acetyl-11-Oxo-olean-12-en-30-oicacid-(2′-dimethylamino) ethyl ester (**12**)

Acetic anhydride (1.0 mL) was added dropwise to a stirred solution of compound **7** (108.4 mg, 0.2 mmol) in pyridine (1.5 mL) at 0 °C. The resulting solution was stirred at rt for 16 h and then poured into ice water (25 mL). The resulting mixture was adjusted to pH 5–6 and extracted with dichloromethane (50 mL × 3). The combined organic layers were washed with water (15 mL × 2) and brine (10 mL), and dried over sodium sulfate. After evaporation of the solvent, the crude residue was purified by column chromatography on silica gel (dichloromethane: methanol = 15: 1) to give the compound **12** (42.8 mg, 37%) as a white solid. ^{1}H NMR (400 MHz, $CDCl_3$) δ 5.68 (s, 1H), 4.52 (dd, J = 11.6, 4.8 Hz, 1H), 4.32 (dt, J = 11.7, 5.9 Hz, 1H), 4.19 (dt, J = 11.7, 5.8 Hz, 1H), 2.87–2.74 (m, 1H), 2.67 (d, J = 4.6 Hz, 2H), 2.36 (s, 6H), 2.21–2.11 (m, 1H), 2.05 (s, 3H), 2.04–1.75 (m, 4H), 1.74–1.54 (m, 5H), 1.49–1.39 (m, 3H), 1.36 (s, 3H), 1.35–1.19 (m, 3H), 1.16 (s, 6H), 1.13 (s, 3H), 1.10–0.96 (m, 3H), 0.88 (s, 6H), 0.80 (s, 3H). ^{13}C NMR (101 MHz, $CDCl_3$) δ 200.9, 176.3, 171.1, 169.4, 128.5, 80.6, 61.7, 57.6, 55.0, 48.2, 45.5, 45.4, 44.0, 43.2, 41.0, 38.8, 38.1, 37.7, 36.9, 32.7, 31.8, 31.1, 28.5, 28.3, 28.1, 26.5, 26.4, 23.6, 23.3, 21.4, 18.7, 17.4, 16.7, 16.4. HRMS (ESI) Calcd. for $C_{36}H_{58}NO_5^+$ ([M+H]$^+$) 584.4315, Found 584.4286.

4.7.12. 18β-3-O-(β-Carboxypropionyl)-11-oxo-olean-12-en-30-oic acid ethyl ester (**13**)

Succinic anhydride (50.0 mg, 0.5 mmol, 5 equiv) and DMAP (24.4 mg, 0.2 mmol, 2.0 equiv) were added to a solution of compound **6** (49.8 mg, 0.1 mmol, 1.0 equiv) in dichloromethane (1 mL) at rt. The resulting solution was stirred at rt for 48 h. Progress of the reaction was monitored by TLC. After completion of the reaction, the mixture was acidified with 1 N HCl to pH ~3 and extracted with ethyl acetate (25 mL × 3). The combined organic layers were washed with water (10 mL) and brine (10 mL), and dried over sodium sulfate. After evaporation of the solvent, the crude residue was purified by column chromatography on silica gel (dichloromethane: methanol = 20: 1) to get the compound **13** (45 mg, 75%) as a white solid. ^{1}H NMR (400 MHz, $CDCl_3$) δ 5.65 (s, 1H), 4.55 (dd, J = 11.7, 4.7 Hz, 1H), 4.28–.98 (m, 2H), 2.80 (dt, J = 13.4, 3.3 Hz, 1H), 2.74–2.59 (m, 4H), 2.36 (s, 1H), 2.15–1.89 (m, 4H), 1.94–1.55 (m, 6H), 1.51–1.38 (m, 3H), 1.37 (s, 3H), 1.34–1.29 (m, 2H), 1.27 (t, J = 7.1 Hz, 3H), 1.23–1.19 (m, 1H), 1.16 (s, 3H), 1.14 (s, 3H), 1.13 (s, 3H),

1.09–0.95 (m, 2H), 0.88 (s, 3H), 0.87 (s, 3H), 0.80 (s, 3H). ^{13}C NMR (101 MHz, CDCl3) δ 200.1, 177.2, 176.4, 171.8, 169.4, 128.5, 81.3, 61.7, 60.3, 55.1, 48.4, 45.4, 43.9, 43.2, 41.1, 38.8, 38.1, 37.7, 37.0, 32.7, 31.8, 31.1, 29.4, 28.9, 28.6, 28.3, 28.0, 26.5, 26.4, 23.5, 23.4, 18.7, 17.4, 16.7, 16.4, 14.3. HRMS (ESI) Calcd. for $C_{36}H_{55}O_7$ ($[M+H]^+$) 599.3942, Found 599.3901.

*4.7.13. 18β-11-Deoxo-olean-12-en-30-oic acidethyl ester (**14**)*

Anhydrous K_2CO_3 (51.1 mg, 0.37 mmol, 1.0 equiv) and EtBr (41 μL, 0.55 mmol, 1.5 equiv) were added to a solution of compound **2** (167.0 mg, 0.37 mmol, 1.0 equiv) in acetone (15 mL) at rt. The resulting solution was stirred at 35 °C for 48 h. Progress of the reaction was monitored by TLC. After completion of the reaction, the acetone was distilled off. The resulting mixture was diluted with water (15 mL) and extracted with dichloromethane (30 mL × 2). The combined organic layers were washed with brine (10 mL) and dried over sodium sulfate. After evaporation of the solvent, the crude residue was purified by column chromatography on silica gel (petroleum ether: ethyl acetate = 10: 1) to produce the compound **14** (176.4 mg, 98%) as a white solid. ^{1}H NMR (400 MHz, $CDCl_3$) δ 5.26 (s, 1H), 4.30–4.01 (m, 2H), 3.24–3.20 (M, 1H), 2.06–1.83 (m, 6H), 1.82–1.74 (m, 1H), 1.64–1.52 (m, 6H), 1.48–1.39 (m, 3H), 1.38–1.21 (m, 7H), 1.14 (s, 3H), 1.12 (s, 3H), 1.00 (s, 3H), 0.96 (s, 3H), 0.94 (s, 3H), 0.91–0.81 (m, 2H), 0.80 (s, 3H), 0.77 (s,3H), 0.76–0.73 (m, 1H). ^{13}C NMR (101 MHz, $CDCl_3$) δ 177.1, 144.5, 122.5, 79.0, 60.0, 55.2, 48.2, 47.7, 44.1, 42.9, 41.6, 39.8, 38.8, 38.6, 38.4, 37.0, 32.7, 31.9, 31.3, 28.5, 28.2, 28.1, 27.3, 27.0, 26.2, 26.0, 23.5, 18.4, 16.8, 15.6, 15.5, 14.3. HRMS (ESI) Calcd. for $C_{32}H_{52}O_3$ ($[M+H]^+$) 485.3989, Found 485.3994.

*4.7.14. 18β-3-O-(β-Carboxypropionyl)-11-deoxo-olean-12-en-30-oic acid ethyl ester (**15**)*

Succinic anhydride (91.9 mg, 0.5 mmol, 5 equiv) and DMAP (45.0 mg, 0.36 mmol, 2.0 equiv) were added to a solution of compound **14** (89.0 mg, 0.18 mmol, 1.0 equiv) in dichloromethane (2 mL) at rt. The resulting solution was stirred at rt for 48 h. Progress of the reaction was monitored by TLC. After completion of the reaction, the mixture was acidified with 1 N HCl to pH 2–3 and extracted with ethyl acetate (30 mL × 3). The combined organic layers were washed with water (15 mL) and brine (15 mL), and dried over sodium sulfate. After evaporation of the solvent, the crude residue was purified by column chromatography on silica gel (dichloromethane: methanol = 20: 1) to give the compound **15** (81 mg, 75%) as a white solid. ^{1}H NMR (400 MHz, $CDCl_3$) δ 5.26 (s, 1H), 4.61–4.43 (m, 1H), 4.29–3.98 (m, 2H), 2.69–4.24 (m, 4H), 2.03–1.82 (m, 6H), 1.80–1.74 (m, 1H), 1.69–1.47 (m, 7H), 1.47–1.38 (m, 1H), 1.37–1.21 (m, 8H), 1.14 (s, 3H), 1.12 (s, 3H), 1.09–0.99 (m, 2H), 0.96 (s, 6H), 0.83–0.87 (m, 8H), 0.78 (s, 3H); ^{13}C NMR (101 MHz, $CDCl_3$) δ 177.2, 171.9, 144.6, 122.4, 81.6, 60.0, 55.3, 48.2, 47.56, 44.1, 42.8, 41.5, 39.8, 38.3, 38.2, 37.8, 36.8, 32.6, 31.9, 31.3, 29.4, 28.8, 28.5, 28.2, 28.0, 27.0, 26.2, 25.9, 23.5, 18.2, 16.8, 16.7, 15.5, 14.3. HRMS (ESI) Calcd. for $C_{36}H_{55}O_6^-$ ($[M-H]^-$) 583.3999, Found 583.3998.

Acknowledgements

This work was supported by the National S&T Major Projects of China (2012ZX09501001, 2012ZX09506001, 2012ZX10002011), the National Basic Research Program of China (2013CB531805), and NSF of China (81573501, 81473181, 81302793).

Appendix A. Supplementary data

Supplementary data related to this article can be found at http://dx.doi.org/10.1016/j.ejmech.2016.02.020

References

[1] T. Satoh, M. Hosokawa, The mammalian carboxylesterases: from molecules to functions, Annu. Rev. Pharmacol. Toxicol. 38 (1998) 257–288.
[2] M.R. Redinbo, P.M. Potter, Mammalian carboxylesterases: from drug targets to protein therapeutics, Drug Discov. Today 10 (2005) 313–325.
[3] S. Bencharit, C.C. Edwards, C.L. Morton, E.L. Howard-Williams, P. Kuhn, P.M. Potter, M.R. Redinbo, Multisite promiscuity in the processing of endogenous substrates by human carboxylesterase 1, J. Mol. Biol. 363 (2006) 201–214.
[4] P.M. Potter, R.M. Wadkins, Carboxylesterases-detoxifying enzymes and targets for drug therapy, Curr. Med. Chem. 13 (2006) 1045–1054.
[5] M. Hosokawa, Structure and catalytic properties of carboxylesterase isozymes involved in metabolic activation of prodrugs, Molecules 13 (2008) 412–431.
[6] C.E. Wheelock, B.M. Phillips, B.S. Anderson, J.L. Miller, M.J. Miller, B.D. Hammock, Applications of carboxylesterase activity in environmental monitoring and toxicity identification evaluations (TIEs), Rev. Environ. Contam. Toxicol. 195 (2008) 117–178.
[7] T. Satoh, P. Taylor, W.F. Bosron, S.P. Sanghani, M. Hosokawa, B.N. La Du, Current progress on esterases: from molecular structure to function, Drug Metab. Dispos. 30 (2002) 488–493.
[8] S.P. Sanghani, P.C. Sanghani, M.A. Schiel, W.F. Bosron, Human carboxylesterases: an update on CES1, CES2 and CES3, Protein Pept. Lett. 16 (2009) 1207–1214.
[9] T. Imai, Human carboxylesterase isozymes: catalytic properties and rational drug design, Drug Metab. Pharmacokinet. 21 (2006) 173–185.
[10] M.J. Hatfield, L. Tsurkan, M. Garrett, T.M. Shaver, J.L. Hyatt, C.C. Edwards, L.D. Hicks, P.M. Potter, Organ-specific carboxylesterase profiling identifies the small intestine and kidney as major contributors of activation of the anticancer prodrug CPT-11, Biochem. Pharmacol. 81 (2011) 24–31.
[11] M.K. Ross, J.A. Crow, Human carboxylesterases and their rolein xenobiotic and endobioticmetabolism, J. Biochem. Mol. Toxicol. 21 (2007) 187–196.
[12] S.E. Pratt, S. Durland-Busbice, R.L. Shepard, K. Heinz-Taheny, P.W. Iversen, A.H. Dantzig, Humancarboxylesterase-2 hydrolyzes the prodrug of gemcitabine (LY2334737) and confers prodrug sensitivity to cancer cells, Clin. Cancer Res. 19 (2013) 1159–1168.
[13] M.K. Ma, H.L. McLeod, Lessons learned from the irinotecan metabolic pathway, Curr. Med. Chem. 10 (2003) 41–49.
[14] S.P. Sanghani, S.K. Quinney, T.B. Fredenburg, Z. Sun, W.I. Davis, D.J. Murry, O.W. Cummings, D.E. Seitz, W.F. Bosron, Carboxylesterases expressed in human colon tumor tissue and their role in CPT-11 hydrolysis, Clin. Cancer Res. 9 (2003) 4983–4991.
[15] K. Takasuna, T. Hagiwara, K. Watanabe, S. Onose, S. Yoshida, E. Kumazawa, E. Nagai, T. Kamataki, Optimal antidiarrhea treatment for antitumor agent irinotecan hydrochloride (CPT-11)-induced delayed diarrhea, Cancer Chemother. Pharmacol. 58 (2006) 494–503.
[16] S.P. Sanghani, S.K. Quinney, T.B. Fredenburg, W.I. Davis, D.J. Murry, W.F. Bosron, Hydrolysis of irinotecan and its oxidative metabolites, 7-ethyl-10- [4-N-(5-aminopentanoic acid)-1-piperidino] carbonyloxycamptothecin and 7-ethyl-10-[4-(1-piperidino)-1-amino] -carbonyloxycamptothecin, by human carboxylesterases CES1A1, CES2, and a newly expressed carboxylesterase isoenzyme, CES3, Drug Metab. Dispos. 32 (2004) 505–511.
[17] R.M. Wadkins, J.L. Hyatt, K.J. Yoon, C.L. Morton, R.E. Lee, K. Damodaran, P. Beroza, M.K. Danks, P.M. Potter, Discovery of novel selective inhibitors of human intestinal carboxylesterase for the amelioration of irinotecan-induced diarrhea: synthesis, quantitative structure-activity relationship analysis, and biological activity, Mol. Pharmacol. 65 (2004) 336–343.
[18] J.L. Hyatt, L. Tsurkan, M. Wierdl, C.C. Edwards, M.K. Danks, P.M. Potter, Intracelluar inhibition of carboxylesterases by benzil: modulation of CPT-11 cytotoxicity, Mol. Cancer Ther. 5 (2006) 2281–2288.
[19] H. Gu, L. Gong, J. Yu, Measurement and comparison of glycyrrhizicacid contents in root of licorice (*Glycyrrhiza uralensis* fisch) from different cultivating areas, J. For. Res. 13 (2002) 141–143.
[20] V. Sharma, R.C. Agrawal, *Glycyrrhiza glabra*-a plant for the future, Mintage, J. Pharm. Med. Sci. 2 (2013) 15–20.
[21] H. Sheng, H. Sun, Synthesis, biology and clinical significance of pentacyclic triterpenes: a multi-target approach to prevention and treatment of metabolic and vascular diseases, Nat. Prod. Rep. 28 (2011), 543–493.
[22] J. Tatsuzaki, M. Taniguchi, K.F. Bastow, K. Nakagawa-Goto, S.L. Morris-Natschke, H. Itokawa, K. Baba, K.H. Lee, Anti-tumoragents 255: novel glycyrrhetinic acid-dehydrozingerone conjugates as cytotoxic agents, Bioorg. Med. Chem. 15 (2007) 6193–6199.
[23] K. Kalani, V. Kushwaha, R. Verma, P.K. Murthy, S.K. Srivastava, Glycyrrhetinic acid and its analogs: a new class of antifilarial agents, Bioorg. Med. Chem. Lett. 23 (2013) 2566–2570.
[24] S. Schwarz, B. Siewert, N.M. Xavier, A.R. Jesus, A.P. Rauter, R. Csuk, A l"natural" approach: Synthesis and cytoxicity of monodesmosidic glycyrrhetinic acid glycosides, Eur. J. Med. Chem. 72 (2014) 78–83.
[25] V.V. Grishko, N.V. Galaiko, I.A. Tolmacheva, I.I. Kucherov, V.F. Eremin, E.I. Boreko, O.V. Savinova, P.A. Slepukhin, Functionalization, cyclization and antiviral activity of A-secotriterpenoids, Eur. J. Med. Chem. 83 (2014) 601–608.
[26] D. Rodríguez-Hernández, A.J. Demuner, L.C.A. Barbosa, R. Csuk, L. Heller, Hederagenin as a triterpene template for the development of new antitumor

compounds, Eur. J. Med. Chem. 105 (2015) 57–62.
[27] M.H. Moon, J.K. Jeong, Y.J. Lee, J.W. Seol, D.C. Ahn, I.S. Kim, S.Y. Park, 18β-Glycyrrhetinic acid inhibits adipogenic differentiation and stimulates lipolysis, Biochem. Biophys. Res. Commun. 420 (2012) 805–810.
[28] C.M. Ku, J.Y. Lin, Anti-inflammatory effects of 27 selected terpenoid compounds tested through modulating Th1/Th2 cytokine secretion profiles using murine primary splenocytes, Food Chem. 141 (2013) 1104–1113.
[29] S.K. Hasan, R. Khan, N. Ali, A.Q. Khan, M.U. Rehman, M. Tahir, A. Lateef, S. Nafees, S.J. Mehdi, S. Rashid, A. Shahid, S. Sultana, 18-β Glycyrrhetinic acid alleviates 2-acetyl aminofluorene-induced hepatotoxicity in wistar rats: role in hyperproliferation, inflammation and oxidative stress, Hum. Exp. Toxicol. 34 (2015) 628–641.
[30] B.D. Wallace, H. Wang, K.T. Lane, J.E. Scott, J. Orans, J.S. Koo, M. Venkatesh, C. Jobin, L.A. Yeh, S. Mani, M.R. Redinbo, Alleviating cancer drug toxicity by inhibiting a bacterial enzyme, Science 330 (2010) 831–835.
[31] W. Lam, S. Bussom, F. Guan, Z. Jiang, W. Zhang, E.A. Gullen, S.H. Liu, Y.C. Cheng, The four-herb chinese medicine PHY906 reduces chemotherapy-induced gastrointestinal toxicity, Sci. Transl. Med. 2 (2010) 45–59.
[32] S.H. Liu, Y.C. Cheng, Old formula, new Rx: the journey of PHY906 as cancer adjuvant therapy, J. Ethnopharmacol. 140 (2012) 614–623.
[33] X.Z. Li, S.N. Zhang, S.M. Liu, F. Lu, Recent advances in herbal medicines treating parkinson's disease, Fitoterapia 84 (2013) 273–285.
[34] Y.G. Li, J. Hou, S.Y. Li, X. Lv, J. Ning, P. Wang, Z.M. Liu, G.B. Ge, J.Y. Ren, L. Yang, *Fructus psoraleae* contains natural compounds with potent inhibitory effects towards human carboxylesterase 2, Fitoterapia 101 (2015) 99–106.
[35] D.X. Sun, G.B. Ge, P.P. Dong, Y.F. Cao, Z.W. Fu, R.X. Ran, X. Wu, Y.Y. Zhang, H.M. Hua, Z. Zhao, Z. Fang, Inhibition behavior of fructus psoraleae's ingredients towards human carboxylesterase 1 (hCES1), Xenobiotica 11 (2015) 1–8.
[36] Z.M. Liu, L. Feng, G.B. Ge, X. Lv, J. Hou, Y.F. Cao, J.N. Cui, L. Yang, A highly selective ratiometric fluorescent probe for in vitro monitoring and cellular imaging of human carboxylesterase 1, Biosens. Bioelectron. 57 (2014) 30–35.
[37] J. Wang, E.T. Williams, J. Bourgea, Y.N. Wong, C.J. Patten, Characterization of recombinant human carboxylesterases: fluorescein diacetate as a probe substrate for human carboxylesterase 2, Drug Metab. Dispos. 39 (2011) 1329–1333.
[38] L. Feng, Z.M. Liu, L. Xu, X. Lv, J. Ning, J. Hou, G.B. Ge, J.N. Cui, L. Yang, A highly selective long-wavelength fluorescent probe for the detection of human carboxylesterase 2 and its biomedical applications, Chem. Commun. 50 (2014) 14519–14522.
[39] H. Eng, M. Niosi, T.S. McDonald, A. Wolford, Y. Chen, S.T. Simila, J.N. Bauman, J. Warmus, A.S. Kalgutkar, Utility of The carboxylesterase inhibitor bis-para-nitrophenyl phosphate (BNPP) in the plasma unbound fraction determination for a hydrolytically unstable amide derivative and agonist of the TGR5 receptor, Xenobiotica 40 (2010) 369–380.
[40] Z.Z. Fang, Y.F. Cao, C.M. Hu, M. Hong, X.Y. Sun, G.B. Ge, Y. Liu, Y.Y. Zhang, L. Yang, H.Z. Sun, Structure-inhibition relationship of ginsenosides towards UDP-glucuronosyltransferases (UGTs), Toxicol. Appl. Pharmacol. 267 (2013) 149–154.
[41] W.L. DeLano, The PyMOL Molecular Graphics System, DeLano Scientific, San Carlos, CA, 2002.
[42] R.A. Laskowski, M.B. Swindells, LigPlot+: multiple ligand-protein interaction diagrams for drug discovery, J. Chem. Inf. Model. 51 (2011) 2778–2786.
[43] A.C. Wallace, R.A. Laskowski, Thornton JMLIGPLOT: a program to generate schematic diagrams of protein-ligand interactions, Protein Eng. 8 (1995) 127–134.